THE ASTROPHYSICAL JOURNAL, 456:393–398, 1996 January 1

THE INFLUENCE OF THE TEMPERATURE PROFILE ON THE MAGNETOHYDRODYNAMIC MODES OF A PROMINENCE-CORONA SYSTEM

R. OLIVER AND J. L. BALLESTER
Departament de Física, Universitat de les Illes Balears, E-07071 Palma de Mallorca, Spain
Received 1995 April 28; accepted 1995 July 10

ABSTRACT

To explain the observational evidence gathered during recent years about periodic oscillations in quiescent solar prominences, the modes of oscillation of some theoretical models for solar prominences have been studied. The main drawback of these models is the lack of a realistic temperature profile for the prominence-corona system, which should be obtained from the coupling between magnetostatics and energetics once the physical properties of the prominence and the prominence-corona transition region (PCTR) are known. However, this seems to be far from our present possibilities since there is a lack of knowledge about the physical processes occurring in both.

To make further progress in the study of MHD waves in prominences, we have adopted an "ad hoc" temperature profile that can be adjusted to give different runs of the temperature, from prominence to coronal values. This profile allows us to modify the thickness of the PCTR while modifying the steepness of the temperature variation within it. Also, by including this profile in the model proposed by Poland & Anzer, we are able to construct an equilibrium model for the prominence-corona system and to study the linear, adiabatic MHD waves of such configuration.

Among the results obtained we highlight that the presence of a PCTR does not eliminate the subdivision of modes into hybrid, external, and internal and that its existence is linked to the presence of two temperature plateaus. A change in the thickness of the PCTR produces a modification of the mode frequency and also affects the horizontal velocity component of internal modes by diminishing its amplitude in the prominance region. For a thin PCTR, because of the velocity amplitude inside the prominence, the modes likely to be detected in prominence oscillations are the internal and hybrid ones, although as a consequence of the effect already pointed out, the existence of a thick PCTR could make difficult or even impossible the detection of internal modes.

In summary, our results point out the importance of the PCTR to the oscillations of quiescent solar prominences and to the identification of modes through the amplitudes of the eigenfunctions in the prominence. This indicates the strong need for accurate knowledge of the physical properties of this region, in order to be able to make accurate theoretical predictions about the amplitudes and frequencies of oscillations in quiescent prominences. Probably, that knowledge can be obtained in the near future by means of the UV instruments of the *SOHO* spacecraft.

Subject headings: MHD — Sun: corona — Sun: magnetic fields — Sun: prominences

1. INTRODUCTION

During recent years, observational evidence about the presence of periodic oscillations or waves in solar prominences has been obtained, and it is well summarized in reviews by Tsubaki (1988), Schmieder (1988, 1989), and Vrsnak (1993). These oscillations have been detected mainly in the velocity field and can be classified into three categories: short-period oscillations, having periods of 5 minutes or less, intermediate-period oscillations, between 8 and 20 minutes, and long-period oscillations, the periods of which range mainly between 40 and 90 minutes. Balthasar et al. (1993) have also established the existence of oscillations of very short period (30 s), and although this value has not been confirmed by other observations, it is hard to doubt its reality since it was determined by a simultaneous observation of the prominence with two telescopes.

Oliver et al. (1993) studied the MHD modes of a solar prominence surrounded by a coronal region with a global magnetic configuration and density given by the modified Kippenhahn-Schlüter model proposed by Poland & Anzer (1971). The configuration consists of a cool and dense medium, representing the prominence, embedded in a hot and tenuous plasma, representing the corona, with uniform but different temperatures in both regions. In such a configuration, in which there is a sudden jump of the temperature and density from prominence to coronal values at the interface between the two regions, slow, fast, and Alfvén modes can be classified as internal, external, or hybrid. Oliver et al. (1993) described internal modes as those that do not disappear when the coronal region is removed, external modes as those that do not disappear when the prominence is removed, and hybrid modes as owing their existence to the presence of both media.

Recently, Oliver & Ballester (1995) used the prominence-corona model of Low & Wu (1981) to study the effects of anisothermality on the MHD modes and to determine how a smooth transition region affects the classification of modes reported in Oliver et al. (1993). The temperature run provided by the Low & Wu model, with a smooth transition between the prominence and the corona, is just the opposite of the sharp one used in Oliver et al. (1993), and no evidence for hybrid, external, and internal modes was found. It was then suggested

that this subdivision disappears when the temperature suffers a very smooth transition from prominence to coronal conditions.

Of course, the ideal situation would be to know exactly which are the physical properties of the prominence-corona transition region (PCTR) and then, by use of a full energy equation, to construct a theoretical model with a realistic temperature profile for the prominence-corona system. However, even with an accurate knowledge of the physics of the PCTR, this is not an easy task because of the nonlinearities in the equations and the difficulty of obtaining realistic prominence temperatures and widths (see, e.g., Milne, Priest, & Roberts 1979; Schmitt & Degenhardt 1995).

The physics of the PCTR is now a subject of lively debate (Engvold 1989; Vial 1990; Chiuderi-Drago 1990) because of the discrepancies coming from the observational data. Analyses of EUV and UV lines in quiescent prominences indicate that the PCTR is very thin and similar to the chromosphere-corona transition region (Orrall & Schmahl 1976; Rabin 1986). However, when the PCTR is observed in limb prominences, by means of UV lines, and in filaments by use of radio wavelengths, the physical parameters needed to explain both sets of observations are in disagreement. Those discrepancies can be solved when the dependence of the thermal conduction on the angle between the magnetic field and the direction of the local temperature gradient is taken into account (Chiuderi & Chiuderi-Drago 1991).

As a tool to make further progress in the study of MHD waves in prominences, we have adopted a temperature profile by which a smooth temperature transition from a cool prominence to a hot corona can be achieved. The shape of this "ad hoc" temperature profile is based on observational evidence (Schmahl 1979) and theoretical models (Chiuderi & Chiuderi-Drago 1991; Rovira et al. 1994), and its expression allows variation of the thickness of the PCTR and the steepness of the temperature profile within it. The expression for temperature was next introduced into the Poland-Anzer model, which yields analytic solutions for the equilibrium quantities, and the linear and adiabatic MHD waves of the system were studied.

Our main goals here are to study the influence of the PCTR on the behavior of the modes and eigenfunctions and to ascertain the conditions needed for the existence of the subdivision of modes reported by Joarder & Roberts (1992) and Oliver et al. (1993).

2. BASIC EQUATIONS AND COMPUTATIONAL TOOLS

2.1. *Equilibrium Equations*

The reader is referred to Oliver et al. (1993) for a complete description of the equilibrium configuration. Let us just mention that the prominence and corona are modeled using a generalization of the one-dimensional solution of Kippenhahn & Schlüter (1957), put forward by Poland & Anzer (1971), that allows one to consider a nonuniform temperature distribution. The equilibrium magnetic field lies in the (x, z)-plane, transverse to the prominence sheet, with a constant horizontal component B_{0x}. The vertical magnetic field component and plasma density are given by

$$B_{0z}(x) = B_{z\infty} \tanh\left[\frac{B_{z\infty}}{2B_{0x}}\frac{gf(x)}{R}\right], \tag{1}$$

$$\rho_0(x) = \frac{B_{z\infty}^2}{2\mu R\tilde{T}(x)} \operatorname{sech}^2\left[\frac{B_{z\infty}}{2B_{0x}}\frac{gf(x)}{R}\right]. \tag{2}$$

Moreover, the plasma density at the prominence center, $\rho_0(0)$, is related to the parameter $B_{z\infty}$ by the expression

$$B_{z\infty}^2 = 2\mu R\tilde{T}(0)\rho_0(0)\,. \tag{3}$$

In the above equations we have introduced the new physical variable $\tilde{T}$, defined in terms of the temperature T and mean atomic weight $\tilde{\mu}$:

$$\tilde{T}(x) = \frac{T(x)}{\tilde{\mu}(x)}\,. \tag{4}$$

This variable is used to replace T and $\tilde{\mu}$ in the equilibrium equations, where they always appear in the form $T/\tilde{\mu}$. The pressure can be obtained from equation (2) and the perfect-gas law:

$$p_0 = \rho_0 R\frac{T(x)}{\tilde{\mu}(x)} \equiv \rho_0 R\tilde{T}(x)\,. \tag{5}$$

In addition, the function $f(x)$ in equations (1) and (2) is given by

$$f(x) = \int_0^x \frac{dx'}{\tilde{T}(x')}\,. \tag{6}$$

In the derivation of the equilibrium physical variables no attention was paid to the termal interplay between conduction and heat gains and losses. The temperature is thus a free function of the model. The MHD modes of oscillation of one-temperature and two-temperature isothermal solutions of the Kippenhahn-Schlüter type have already been investigated by Oliver et al. (1992, 1993). We here consider a profile in which there is a smooth temperature transition from a central plateau with prominence conditions to two lateral plateaus with coronal conditions (see Fig. 1*a* for typical plots of $\tilde{T}$). From among the large number of ways in which this could be achieved, we selected the formula

$$\tilde{T}(x) = \frac{1}{2}(\tilde{T}_c + \tilde{T}_p) + \frac{1}{2}(\tilde{T}_c - \tilde{T}_p)\tanh\frac{x - x_m}{\Delta} \tag{7}$$

for $x \geq 0$ and a symmetric counterpart for $x \leq 0$. This expression corresponds to a central prominence region with $\tilde{T}(x) \approx \tilde{T}_p = T_p/\tilde{\mu}_p$ embedded in a coronal region with $\tilde{T}(x) \approx \tilde{T}_c = T_c/\tilde{\mu}_c$. The transition layer between the two regions (i.e., the PCTR) is centered about the positions $x = \pm x_m$ and, for the profile given by equation (7), has a thickness roughly equal to 6Δ.

The values $\tilde{T}_p = 10^4$ K and $\tilde{T}_c = 2 \times 10^6$ K were used in all the computations described here; this is equivalent to taking, for example, a prominence with a temperature $T_p = 7000$ K and $\tilde{\mu} = 0.7$ and a corona with $T_c = 10^6$ K and $\tilde{\mu} = 0.5$. Moreover, the values $B_{0x} = 5$ G and $\rho_0(0) = 5 \times 10^{-11}$ kg m^{-3} have been assumed. Figure 1 shows the temperature and density profiles obtained from equations (7) and (2) for different widths of the PCTR.

2.2. *Magnetoacoustic Wave Equations*

Adiabatic oscillations of the system about the equilibrium state are next considered, which results in a pair of coupled ordinary differential equations for the x- and z-components of the plasma velocity (see Oliver & Ballester 1995):

$$\frac{d^2v_x}{dx^2} = q_1\frac{dv_x}{dx} + q_2\frac{dv_z}{dx} + q_3 v_x + q_4 v_z\,, \tag{8}$$

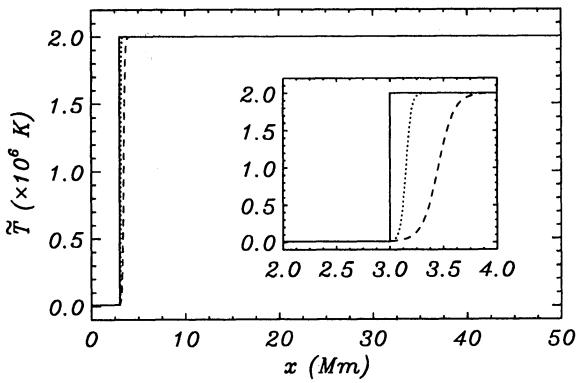

FIG. 1a

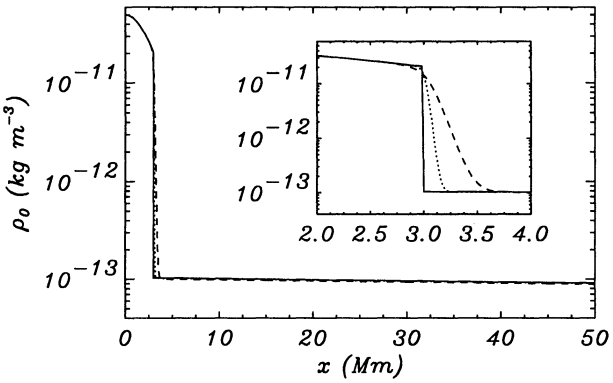

FIG. 1b

FIG. 1.—(*a*) Equilibrium temperature (with $\tilde{T} = T/\tilde{\mu}$) and (*b*) equilibrium density for different widths of the prominence-corona transition region (roughly equal to 6Δ). In these figures $x_m = 3\Delta + 3000$ km and $x_c = 50{,}000$ km. Solid lines: $6\Delta = 0$; dotted lines: $6\Delta = 300$ km; dashed lines: $6\Delta = 900$ km.

$$\frac{d^2 v_z}{dx^2} = q_5 \frac{dv_x}{dx} + q_6 \frac{dv_z}{dx} + q_7 v_x + q_8 v_z , \tag{9}$$

where the coefficients q_1–q_8 are complex functions of x that involve the oscillatory frequency ω and the wavenumber in the vertical direction, k_z. The solutions of these two equations describe the behavior of the fast and slow magnetoacoustic modes of equilibrium models of the Kippenhahn-Schlüter type. The Alfvén mode is governed by a separate equation, decoupled from the previous two, and is not studied here. One of the conclusions in Oliver et al. (1993) and Oliver & Ballester (1995) is that the Alfvén mode has properties very similar to those of fast modes with infinite vertical wavelength (i.e., for $k_z = 0$), and one can reasonably expect that the same will happen in the present situation.

2.3. *Numerical Computations*

Equations (8) and (9) have been integrated between $x = -x_c$ and $x = +x_c$, and at these two places we have assumed the existence of a dense photosphere that acts as a rigid and perfectly conducting wall against coronal perturbations. This means that our differential equations are supplemented with the four boundary conditions

$$v_x(\pm x_c) = v_z(\pm x_c) = 0 . \tag{10}$$

In the numerical computations that we perform, the variables are dedimensionalized as follows:

$$\bar{x} = \frac{x}{x_0} , \quad \bar{z} = \frac{z}{x_0} , \quad \bar{k}_z = k_z x_0 ,$$

$$\bar{v}_x = \frac{v_x}{c_s(0)} , \quad \bar{v}_z = \frac{v_z}{c_s(0)} , \quad \bar{c}_s = \frac{c_s}{c_s(0)} ,$$

$$\bar{B}_{0x} = \frac{B_{0x}}{B_{0x}} \equiv 1 , \quad \bar{B}_{0z} = \frac{B_{0z}}{B_{0x}} , \quad \bar{\rho}_0 = \frac{c_s^2(0)\mu\rho_0}{\gamma B_{0x}^2} , \tag{11}$$

$$\bar{g} = \frac{g x_0}{c_s^2(0)} , \quad \bar{\omega} = \frac{\omega x_0}{c_s(0)} ,$$

where x_0 is a length used for dedimensionalization (for which the value $x_0 = 3000$ km is used), $c_s^2(x) = \gamma RT(x)/\tilde{\mu}(x)$ is the square of the sound speed, and $c_s(0)$ is the sound speed at the prominence center.

One of the effects of gravity on the fast and slow modes of the system is the vertical amplification or damping of waves that results from a complex vertical wavenumber. Here we follow Oliver et al. (1992, 1993) and write $\bar{k}_z = \alpha + i\delta$, i.e., $k_z = \alpha/x_0 + i\delta/x_0$, so that fast and slow waves propagate with a vertical wavelength equal to $2\pi x_0/\alpha$ and their amplitude is modified by the factor $\exp(\delta z/x_0)$. In the solution of equations (8) and (9), we select a fixed value of α and thus have an eigenvalue problem, with $v_x(x)$ and $v_z(x)$ the (complex) eigenfunctions and ω and δ the (real) eigenvalues.

A careful study of the problem posed by equations (8), (9), and (10) shows that the eigenfunctions $v_x(x)$ and $v_z(x)$ are symmetric or antisymmetric about $x = 0$ (in fact, they must have opposite parity), and so the integration of the differential equations can also be carried out between the center of the system ($x = 0$), where knowledge of the parities of v_x and v_z can be used, and the boundary ($x = +x_c$). No difference between the solutions calculated by integrating from $x = -x_c$ to $x = +x_c$ and from $x = 0$ to $x = +x_c$ has been observed; therefore, the second range of integration is used in most of the calculations presented here since it is the one that results in better performance of the numerical codes.

The differential equations were solved with the help of the numerical techniques that are described in Oliver et al. (1992, 1993). The first of these techniques is based on the construction of the solution to equations (8) and (9) as a linear combination of two auxiliary solutions that satisfy the known boundary conditions for v_x and v_z at one end of the integration range. We then have an initial-value problem for the auxiliary solutions, which are propagated toward the other end. At this point, the boundary conditions described by equation (10) yield a constraint that helps us find the eigenvalues ω and δ. The computations carried out in Oliver et al. (1993) prove that this method is often inadequate when large values of the width of the system or the wavenumber are selected, so it has only been used for small x_c and α. For larger values of x_c or α, a boundary-value technique has been used, as it is far more adequate.

3. RESULTS

We first compute the dispersion diagrams for different widths of the transition region (6Δ), with x_m in equation (7) given by $x_m = 3\Delta + 3000$ km. The other parameters are held fixed. These dispersion diagrams are similar to those in previous works (e.g., Figs. 2 and 3 in Oliver et al. 1993 and Fig. 3 in Oliver & Ballester 1995), in that the square of the fast-mode frequency shows a parabolic dependence on wavelength while the frequency of slow modes displays almost no variation with

wavelength. Thus, the results can be well characterized by the value of ω for $\alpha = 0$, that is, for infinite wavelength in the vertical direction.

Tables 1 and 2 show the square of the dimensionless frequency for the kink and sausage modes, respectively, with lowest ω and three values of the PCTR thickness: $6\Delta = 0$, 300, and 900 km. The results indicate that a thin PCTR has almost no influence on the modes of the system, the reason being that the modes under consideration have wavelengths of the order of or larger than 20 Mm and thus "see" the smooth transition region (only 300 or 900 km wide) as a genuine discontinuity, so one should expect only minor differences between the three configurations. Modes with wavelengths of the order of or shorter than the width of the PCTR are those most affected by the inclusion of a transition region between prominence and corona.

The modes in Tables 1 and 2 have been labeled as hybrid, external, and internal. Evidence for this subdivision comes from various features of the modes, one being the evolution of their frequencies, for $\alpha = 0$, as x_c is changed. This frequency evolution is shown in Figure 2 for the case in which no PCTR is present (obviously, no differences were found between this plot and those for $6\Delta = 300$ and 900 km). As the half-width increases in this figure, one can see that external modes (*dotted lines*) are clearly affected by the change in x_c, whereas internal modes (*solid lines*) are practically unaffected, except at the regions where they interact with external modes. It is worth noticing that the coupling between internal and external modes in these diagrams is very weak, so the transformation of a mode from one type to the other takes place over a large range of x_c and is not actually as clear-cut as it appears in Figure 2.

TABLE 1

DIMENSIONLESS FREQUENCY SQUARED OF MAGNETOACOUSTIC KINK MODES

MODE TYPE[a]	$\bar{\omega}^2$ FOR PCTR WIDTH (6Δ)		
	0 km	300 km	900 km
HS	8.90×10^{-2}	8.88×10^{-2}	8.84×10^{-2}
ES1	7.28	7.27	7.25
IS1	11.27	11.17	10.98
ES2	30.60	30.58	30.48
IS2	40.72	40.32	39.50

[a] Key: H = hybrid, E = external, and I = internal; S = slow and F = fast. The numbers 1 and 2 denote first and second harmonic.

TABLE 2

DIMENSIONLESS FREQUENCY SQUARED OF MAGNETOACOUSTIC SAUSAGE MODES

MODE TYPE[a]	$\bar{\omega}^2$ FOR PCTR WIDTH (6Δ)		
	0 km	300 km	900 km
HF	2.18	2.18	2.16
IS1	3.61	3.58	3.54
ES1	7.92	7.92	7.92
IS2	22.46	22.23	21.75
ES2	31.84	31.83	31.82

[a] Key: H = hybrid, E = external, and I = internal; S = slow and F = fast. The numbers 1 and 2 denote first and second harmonic.

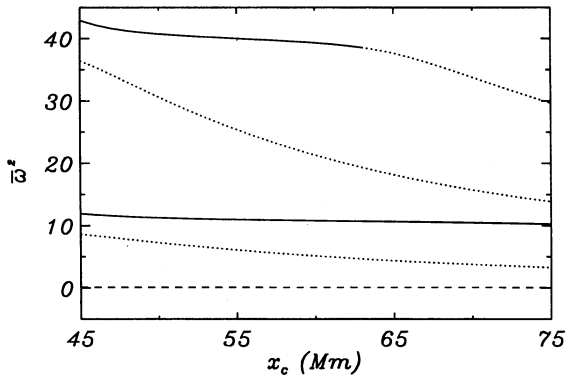

FIG. 2.—Dimensionless frequency squared ($\bar{\omega}^2$) of kink modes vs. the half-width of the system (x_c) for a configuration without PCTR ($6\Delta = 0$).

The behavior of the modes in Figure 2 can be understood with the analysis of the frequencies of a simpler system, such as the one studied by Joarder & Roberts (1992), obtained by removing the PCTR in the temperature profile and eliminating the vertical magnetic field component, which results in a uniform prominence and a uniform corona. The approximate values of the frequency (see eqs. [54] and [55] in Oliver et al. 1993) predict $\omega \propto x_c^{-1}$ for external modes, $\omega \propto x_c^{-1/2}$ for hybrid modes, and ω independent of x_c for internal modes.

In order to obtain further clarification of the nature of internal, external, and hybrid modes, we consider two additional types of temperature profile computed from equation (7): one in which a very thin prominence is embedded in a coronal environment and a second in which a normal-sized prominence is surrounded by a very narrow layer of hotter plasma. Following the idea that led to plotting Figure 2, the frequency of magnetoacoustic modes has been plotted versus x_c for $\alpha = 0$ (see Figs. 3*a* and 3*b*). It is obvious that all modes evolve in a similar way and that their relative positioning is maintained as the half-width is varied. It is therefore impossible to make any differentiation among the different modes in Figures 3*a* and 3*b*, which then leads us to the conclusion that the distinction between internal, external, and hybrid modes is meaningless in a configuration in which either the prominence or the corona is practically eliminated. We conclude that, in order to have the three types of modes (internal, external, and hybrid), the coexistence of two different regions with quite different temperatures is necessary. After an almost complete removal of one of the regions, we are left with the modes belonging to the resultant inhomogeneous region, which evolve similarly to one another when x_c is varied.

Another effect that has important observational consequences is the modification of the shape of the horizontal velocity component for the internal modes, the amplitude of which suffers a reduction in the prominence region. When the thickness of the PCTR is small, the order of magnitude of the amplitude of the horizontal component of the eigenfunction is similar in the prominence and the corona, but when the thickness is increased the amplitude outside the prominence becomes much greater than inside, as for external modes. This indicates that the presence of a thick PCTR will make difficult the detection of the internal modes in the body of the prominence, limiting the possibility of detection to hybrid modes, whose eigenfunctions are unaffected by the thickness of the PCTR. On the other hand, the eigenfunctions corresponding to external modes are also unaffected by changes in the thickness of the PCTR.

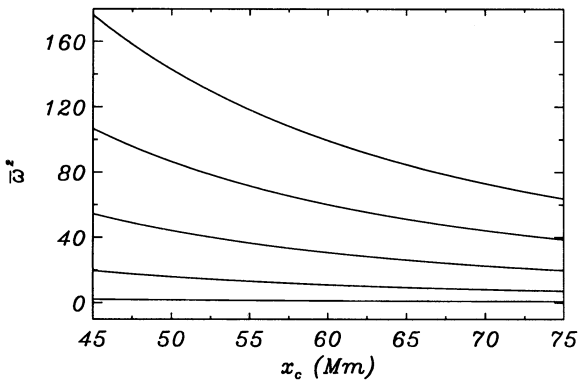

FIG. 3*a*

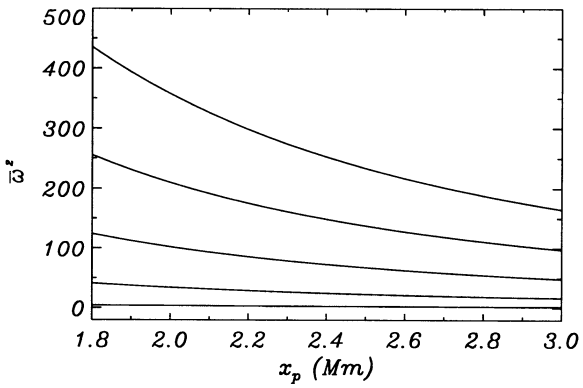

FIG. 3*b*

FIG. 3.—Dimensionless frequency squared ($\bar{\omega}^2$) of kink modes vs. (*a*) the half-width (x_c) for a system with a very narrow prominence region and (*b*) the prominence half-width (x_p) for a system without coronal region. The temperature profiles were computed from eq. (7) with (*a*) $\Delta = 1.5$ km and $x_m = 4.5$ km and (*b*) $\Delta = 150$ km, $x_m = x_c - 50$ km, and $x_p = x_c - 500$ km.

4. CONCLUSIONS

In this paper, we have studied the influence a PCTR has on the MHD modes of oscillation of a quiescent prominence. This study was performed by inclusion of an "ad hoc" temperature profile in the model put forward by Poland & Anzer (1971). A temperature profile was chosen so that its steepness within the PCTR and the width of the PCTR could be varied at the same time. Once the model was set up, we studied the linear, adiabatic MHD modes of such configuration.

Our main results can be summarized as follows:

1. Hybrid, external, and internal modes have been found for the widths of the PCTR considered, i.e., up to 900 km.
2. The identification of such modes can be made easily by studying the frequency change when the system's boundary position (x_c) is modified. Change in x_c gives rise to different frequency shifts for the different types of modes, in agreement with the results in Joarder & Roberts (1992) and Oliver et al. (1993).
3. The frequency is influenced by the thickness of the transition region; it always decreases when the thickness is increased. However, this influence is greater for the harmonics since they have shorter wavelengths.
4. When the coronal region is removed, leaving the prominence and the transition regions, the distinction between the different modes disappears, and we are left with the modes corresponding to the remaining, inhomogeneous region.
5. The same happens when the cool region with constant temperature is made very narrow while keeping the transition and coronal regions. This situation corresponds to the theoretical temperature profiles computed by Chiuderi & Chiuderi-Drago (1991) and Rovira et al. (1994).
6. In a previous paper (Oliver et al. 1993), it was shown that internal modes have a horizontal velocity that is greater in the prominence than in the corona, which led to the conclusion that internal and hybrid modes are the most likely to be detected. In the present case, this holds true when the thickness of the PCTR is small, but when this thickness is increased, the horizontal velocity component of internal modes becomes very similar to that of external modes, as its maximum is now found in the corona. On the other hand, the shape of the hybrid-mode eigenfunction remains basically unchanged. Of course, this has important observational consequences since the possibility of detection of internal modes will diminish proportionally to the thickness of the PCTR.

The most important consequence of the above results is that the existence of the subdivision of modes is due to the coexistence of two media, connected by the PCTR, with two different plateaus of temperature. The removal of one of such plateaus leads automatically to the disappearance of the subdivision.

We also have shown that the presence of a PCTR can affect substantially the modes of oscillation of prominences by varying their frequencies and, in some cases, modifying the eigenfunctions. All this evidence points out how crucial it is to obtain an accurate knowledge of the physical properties of the PCTR (i.e., whether it is a continuous or a discrete structure, the temperature and density profiles, its typical thickness, etc.), not only to understand the gathered observational data on prominence oscillations and to make accurate theoretical predictions, but also to be able to construct realistic models of quiescent prominences. Hopefully, we expect that, in the near future, such information about the PCTR will be obtained by means of UV instruments on board the *SOHO* spacecraft.

We would like to acknowledge the financial support received from DGICYT PB93-0420.

REFERENCES

Balthasar, H., Wiehr, E., Schleicher, H., & Wöhl, H. 1993, A&A, 277, 635
Chiuderi, C., & Chiuderi-Drago, F. 1991, Sol. Phys., 132, 81
Chiuderi-Drago, F. 1990, in IAU Colloq. 117, Dynamics of Quiescent Prominences, ed. V. Ruzdjak & E. Tandberg-Hanssen (Heidelberg: Springer), 70
Engvold, O. 1989, in Dynamics and Structure of Quiescent Solar Prominences, ed. E. R. Priest (Dordrecht: Kluwer), 47
Joarder, P. S., & Roberts, B. 1992, A&A, 261, 625
Kippenhahn, R., & Schlüter, A. 1957, Z. Astrophys., 43, 36
Low, B. C., & Wu, S. T. 1981, ApJ, 248, 335
Milne, A. M., Priest, E. R., & Roberts, B. 1979, ApJ, 232, 304
Oliver, R., & Ballester, J. L. 1995, ApJ, 448, 444
Oliver, R., Ballester, J. L., Hood, A. W., & Priest, E. R. 1992, ApJ, 400, 369
———. 1993, ApJ, 409, 809
Orrall, F. Q., & Schmahl, E. J. 1976, Sol. Phys., 50, 365
Poland, A., & Anzer, U. 1971, Sol. Phys., 19, 401
Rabin, D. 1986, in Coronal and Prominence Plasmas, ed. A. I. Poland (NASA CP-2442) (Springfield, VA: NASA), 135
Rovira, M. G., Fontenla, J. M., Vial, J. C., & Gouttebroze, P. 1994, in IAU Colloq. 144, Solar Coronal Structures, ed. V. Rusin, P. Heinzel, & J. C. Vial (Tatranská Lomnica, The Slovak Republic: Slovak Acad. Sci.), 315

Schmahl, E. J. 1979, in IAU Colloq. 44, Physics of Solar Prominences, ed. E. Jensen, P. Maltby, & F. Q. Orrall (Oslo: Inst. Teor. Astrophys.), 102
Schmieder, B. 1988, in Dynamics and Structure of Solar Prominences, ed. J. L. Ballester & E. R. Priest (Palma de Mallorca: Univ. Illes Balears), 10
———. 1989, in Dynamics and Structure of Quiescent Solar Prominences, ed. E. R. Priest (Dordrecht: Kluwer), 37
Schmitt, D., & Degenhardt, U. 1995, in Rev. Mod. Astron. (Heidelberg: Springer), in press
Tsubaki, T. 1988, in Solar and Stellar Coronal Structures and Dynamics, ed. R. C. Altrock (Sunspot, NM: Natl. Sol. Obs.), 140
Vial, J. C. 1990, in IAU Colloq. 117, Dynamics of Quiescent Prominences, ed. V. Ruzdjak & E. Tandberg-Hanssen (Heidelberg: Springer), 106
Vrsnak, B. 1993, Hvar Obs. Bull., 17, 23